**Supporting Information**

## Compositional engineering of multicomponent garnet scintillators: Towards an ultra-accelerated scintillation response.

Lorris Martinazzoli[1,2], Saulius Nargelas[3], Pavel Boháček[4], Roberto Cala'[1,2], Michal Dusek[5], Jan Rohlicek[5], Gintautas Tamulaitis[3], Etiennette Auffray[1], Martin Nikl[5]*

[1]CERN, CH-1211 Geneva 23, Switzerland
[2]Universitá degli Studi di Milano-Bicocca, 20126 Milano, Italy
[3]Institute of Photonics and Nanotechnology, Vilnius University, 10257 Vilnius, Lithuania
[4]Institute of Physics of the Czech Academy of Sciences, 18200 Prague, Czech Republic
[5]Institute of Physics of the Czech Academy of Sciences, 16200 Prague, Czech Republic

*corresponding author: nikl@fzu.cz, ph. +420 220318445

The XRD analysis performed in the crystal ingot at the end part adjacent to the position of AL6 did not reveal any parasitic phases, Fig. S1. Presence of two identical cubic garnet structures slightly differing in the lattice constant might indicate the presence of micron-scale regions with two certain Al/Ga ratio which has been discussed in literature[1], and the results obtained in the present work might be an experimental confirmation.
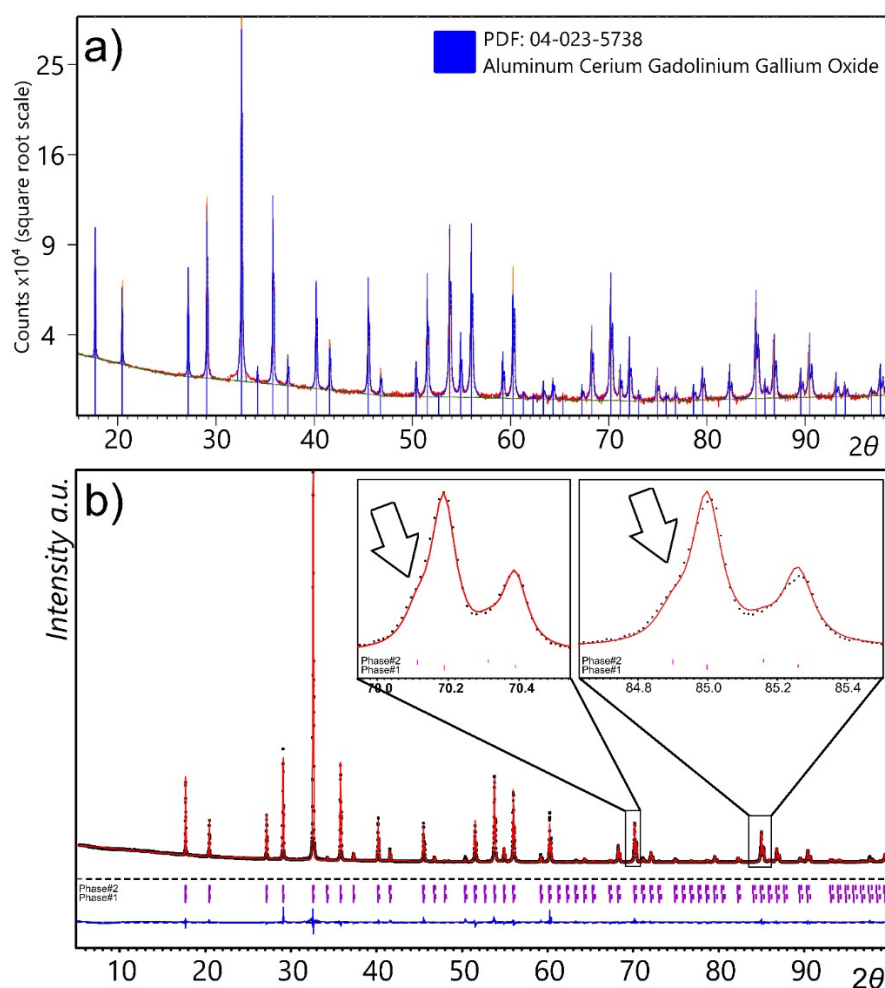


Fig. S1 XRD in the Bragg-Brentano arrangement (λ=CuKα) from 5 to 100° 2θ, step 0.013° 2θ, at the total measurement time of 18h: a) correspondence to the cubic garnet structure matching the PDF card no. 04-023-5738, b) result of the Rietveld refinement using two

identical cubic garnet structures slightly differing in the unit cell parameter *a*. In the insets: two relatively high-intensity peaks at high 2θ angle selected to show peak-splitting.

To provide a visual comparison of decay acceleration and increasing non-exponentiality along the series of PL samples, their room-temperature photoluminescence decays approximated by a sum of two exponentials are displayed in Fig. S2.
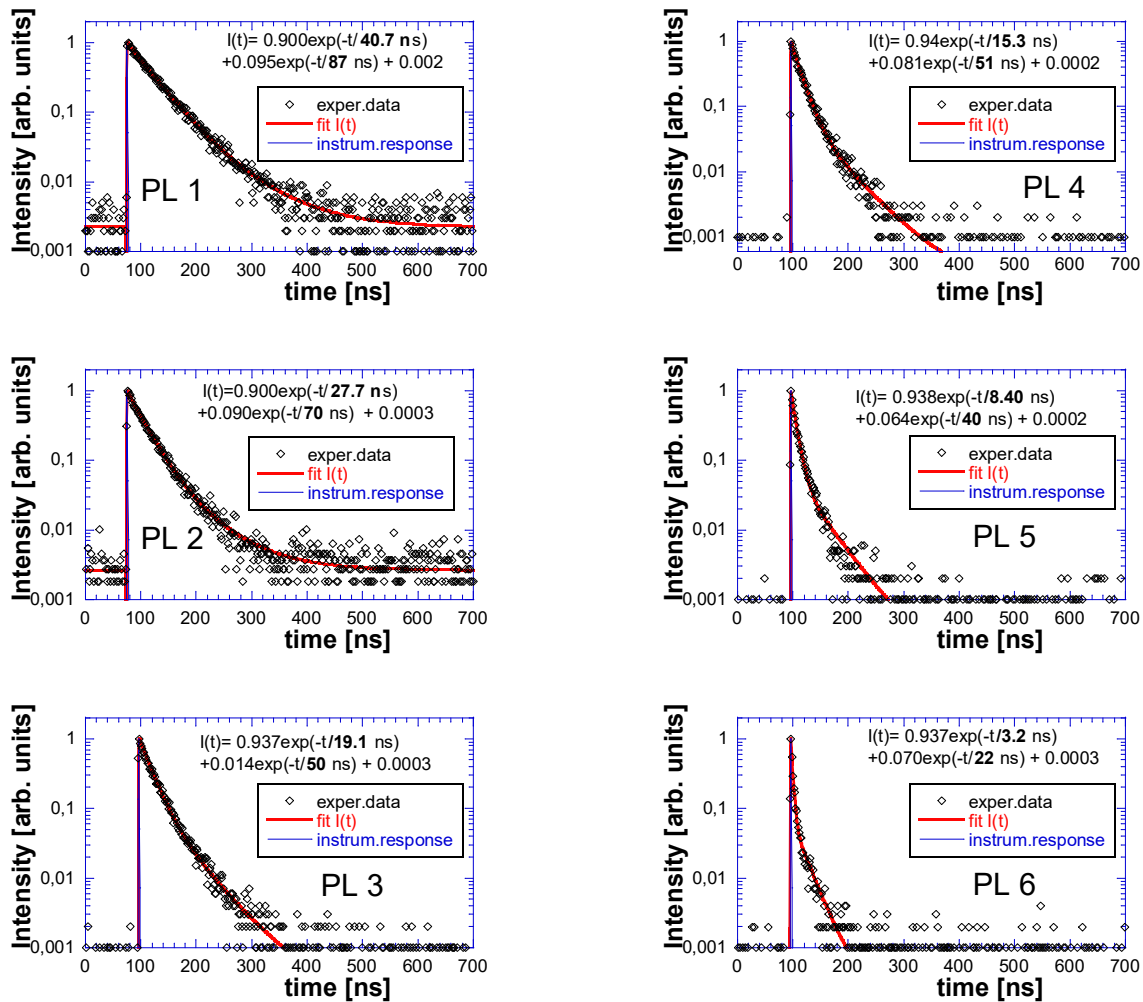


Fig. S2 Photoluminescence decay in samples PL1 - PL6 (points) and its approximation by a biexponential function *I(t)* provided in the plot by red solid lines which are the convolution of instrumental response (presented by blue line) with the function *I(t)*.

Photoluminescence decay kinetics at different temperatures are shown for samples PL 1 and PL 6 in Fig. S3.
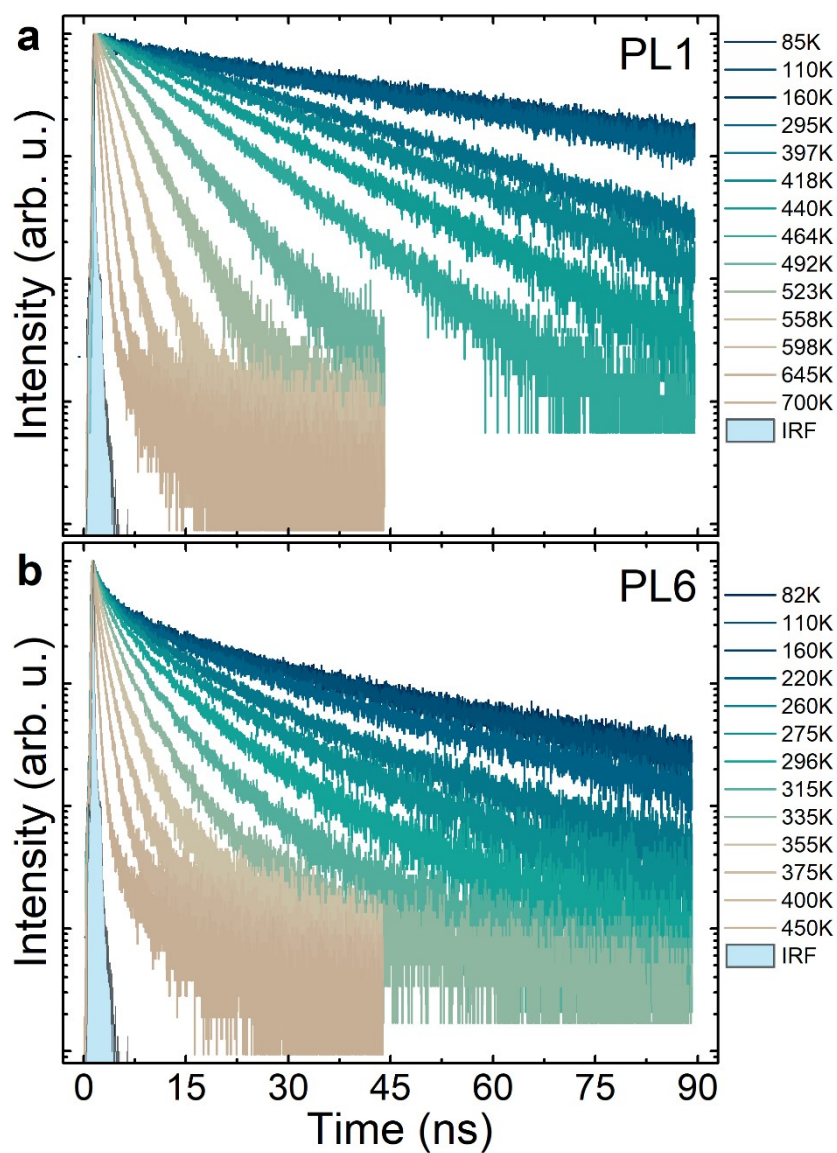


Fig. S3 Time evolution of normalized spectrally-integrated photoluminescence intensity of samples PL1 and PL6 at different temperatures (indicated).

Normalized scintillation decay kinetics measured at excitation by 511 keV using radioisotope
[22]Na at room temperature for all studied samples PL1 – PL6 are shown in Fig. S4. Figure S5
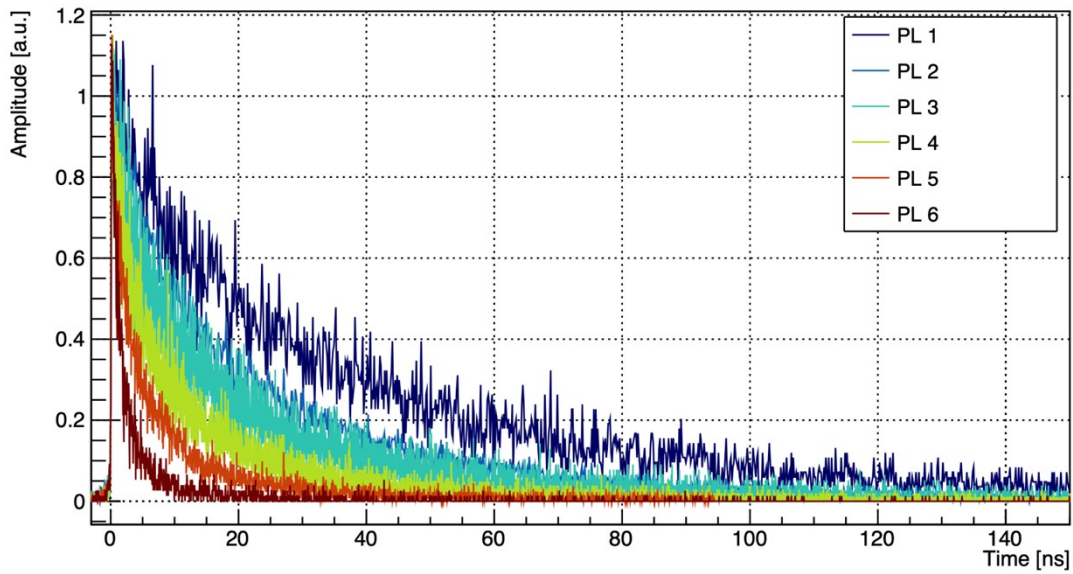shows the initial part of the decay.



Fig. S4 Scintillation decay kinetics in the set of samples PL1 – PL6 after excitation by 511
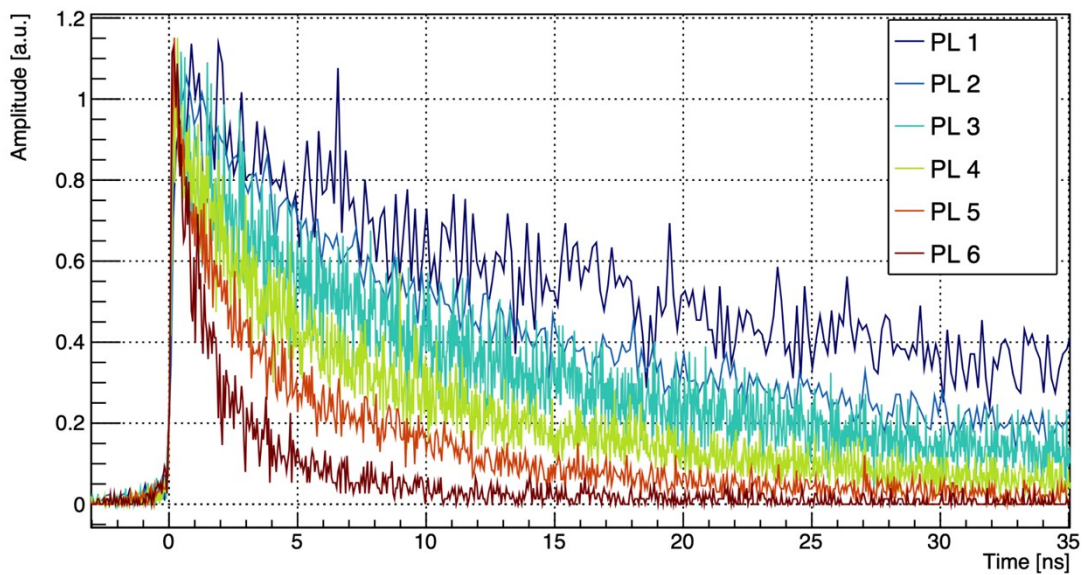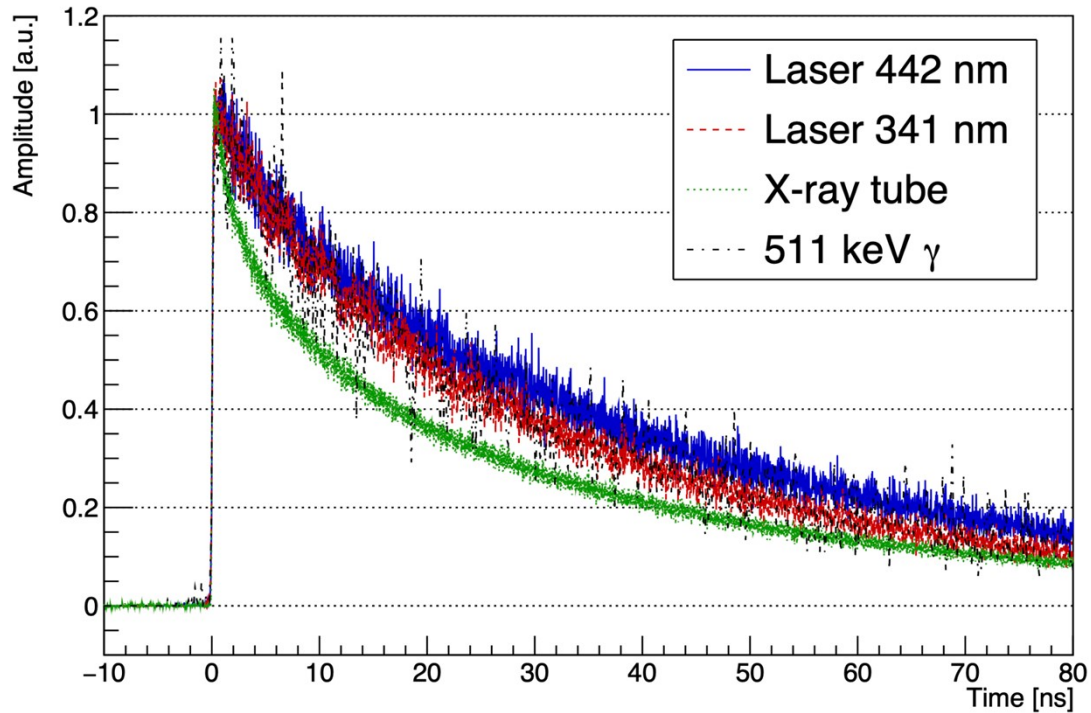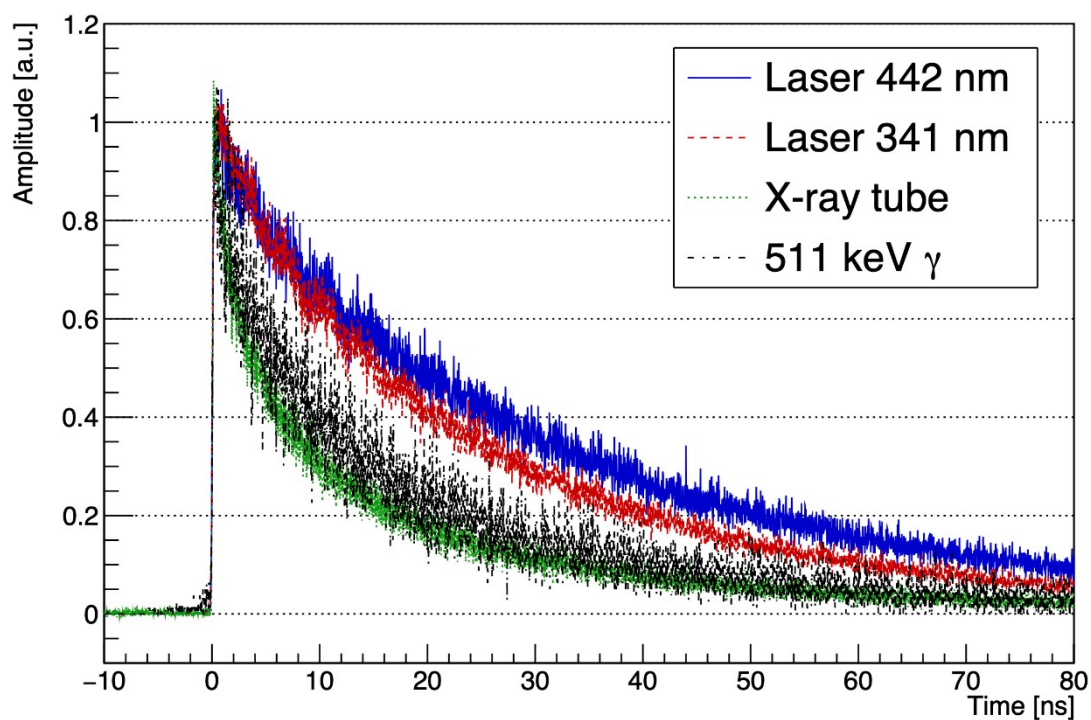keV photons.



Fig. S5 Initial part of scintillation decay kinetics in the set of samples PL1 – PL6 after
excitation by 511 keV photons.

Luminescence decay kinetics after excitation by 511 keV gamma photons, short X-ray pulses and laser pulses at 341 and 442 nm are measured in all samples under study and are presented for samples PL2, PL3, PL 4 and PL5 in Fig. S6. All the decays become substantially faster with increasing doping level.
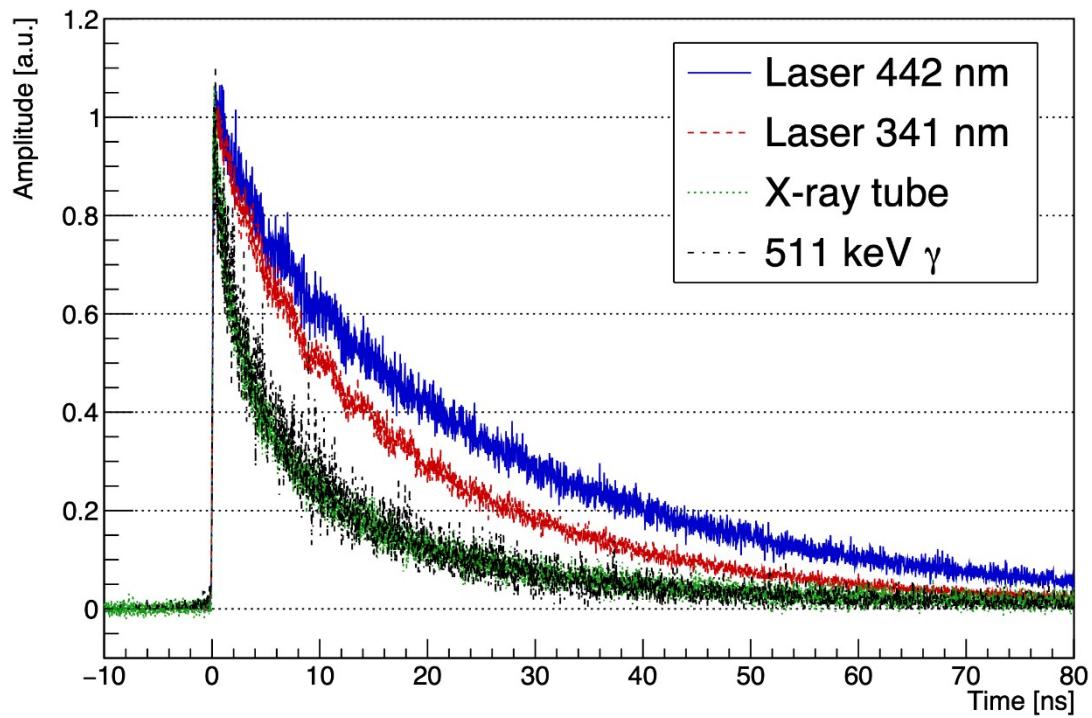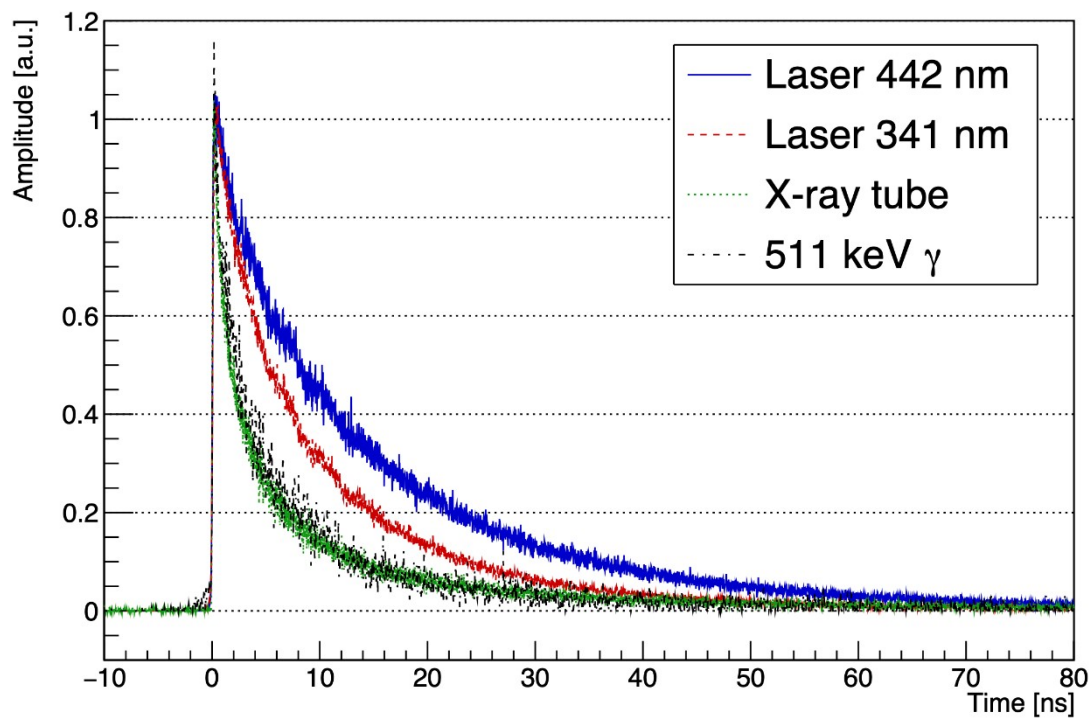
Fig. S6 Kinetics of normalized luminescence decay after excitation by 511 keV gamma photons, short X-ray pulses and laser pulses at 341 and 442 nm in samples PL2, PL3, and PL5 (indicated).

Table S1: Scintillation rise time ($\tau_r$) and decay times ($\tau_{d1}$, $\tau_{d2}$, $\tau_{d3}$) of three components with corresponding relative intensities $R_1$, $R_2$, $R_3$ measured in 1x1x5 mm³ samples PL1 – PL6 after excitation by 511 keV photons. $\tau_{d,eff}$ is defined by eq. (2) in the main text. The uncertainty is 25 ps and 5% for the rise and decay times, respectively.

| Sample | $\tau_r$ [ps] | $\tau_{d1}$ [ns] | $R_1$ % | $\tau_{d2}$ [ns] | $R_2$ % | $\tau_{d3}$ [ns] | $R_3$ % | $\tau_{d,eff}$ [ns] |
|--------|--------|--------|--------|--------|--------|--------|--------|--------|
| PL 1 | 63 | 24.8 | 44.6 | 77.5 | 55.4 | - | - | 40 |
| PL 2 | 0 | 3.0 | 5.4 | 21.3 | 64.5 | 76 | 30.1 | 19.1 |
| PL 3 | 0 | 2.3 | 4.4 | 15.2 | 52.6 | 52 | 43.0 | 16.1 |
| PL 4 | 0 | 2.3 | 10.7 | 12.4 | 60.8 | 55 | 28.5 | 9.9 |
| PL 5 | 0 | 1.2 | 11.1 | 6.8 | 55.9 | 36 | 33.0 | 5.5 |
| PL 6 | 0 | 0.4 | 1.5 | 1.7 | 56.6 | 15 | 41.9 | 2.4 |

1. O. Sidletskiy, Trends in Search for Bright Mixed Scintillators. *Phys. Status Solidi A* 2018, 215, 1701034